Journal of Power Sources 244 (2013) 561–564

Contents lists available at SciVerse ScienceDirect

Journal of Power Sources

journal homepage: www.elsevier.com/locate/jpowsour

Short communication

Electrochemical properties of transition metal substituted calcium ferrite-type $Li_x(M_{0.1}Mn_{0.9})_2O_4$ (M = Ni, Ti)

Mikito Mamiya [a,*], Kunimitsu Kataoka [a], Junji Akimoto [a], Shu Kikuchi [b], Yuka Terajima [b], Kazuyasu Tokiwa [b]

[a] National Institute of Advanced Industrial Science and Technology (AIST), Tsukuba Central 5, 1-1-1 Higashi, Tsukuba, Ibaraki 305-8565, Japan
[b] Department of Applied Electronics, Tokyo University of Science, 2461 Yamazaki, Noda-shi, Chiba 278-8510, Japan

HIGHLIGHTS

- New crystal phase of calcium ferrite-type $Li_x(M_{0.1}Mn_{0.9})_2O_4$ (M = Ni, Ti) are synthesized.
- The crystal structures are revealed by X-ray powder diffraction data.
- The electrochemical properties show high energy densities and good cycle performances.
- Transition metals substitute the Mn sites selectively.
- Different substitution sites show different electrochemical properties.

ARTICLE INFO

Article history:
Received 31 October 2012
Received in revised form
17 January 2013
Accepted 28 January 2013
Available online 5 February 2013

Keywords:
Lithium manganese oxide
Positive electrode
High-pressure
Ion exchange
$CaFe_2O_4$-type
Crystal structure

ABSTRACT

Transition metal substituted $CaFe_2O_4$-type $Li_x(M_{0.1}Mn_{0.9})_2O_4$ (M = Ni, Ti) was synthesized by Na/Li ion exchange method from high-pressure synthesized $CaFe_2O_4$-type $Na(M_{0.1}Mn_{0.9})_2O_4$ (M = Ni, Ti). The crystal structures were refined by Rietveld analysis using powder X-ray diffraction data. The electrochemical properties were measured. The initial discharge capacities of $Li_x(Ni_{0.1}Mn_{0.9})_2O_4$ and $Li_x(Ti_{0.1}Mn_{0.9})_2O_4$ were 119.3 and 122.0 mAh g^{-1} in the range of 4.8–3.0 V (vs Li/Li+). The capacities of substitutions were 5.29% and 7.68% increased than the value of $Li_{0.81}Mn_2O_4$. After 50 charge–discharge cycles, the discharge capacities of $Li_{0.81}Mn_2O_4$ and $Li_x(Ni_{0.1}Mn_{0.9})_2O_4$ were 5.78% and 11.1% decreased from the initial. The Ni substitution was effective for increasing the discharge voltage, although the effect was decreased with increasing cycle numbers.

1. Introduction

Lithium manganese oxides having the layered rocksalt-type and spinel-type structures are very attractive as positive electrode materials in rechargeable lithium batteries, because of their economical and environmental advantages [1]. Among them, spinel-type $LiMn_2O_4$ and its derivatives are the most promising candidate, since this compound can be reversibly deintercalated and intercalated by lithium ions at high potential. An electrochemical cell with spinel-type lithium manganese oxides has an achievable electrode capacity of 100–120 mAh g^{-1} at an average voltage of 4 V vs Li/Li^+. However, the capacity cannot exceed the Li-ion intercalation limit of the spinel crystal structure (theoretical capacity: 148 mAh g^{-1}).

In mineralogy, the spinal-type to $CaFe_2O_4$-type transformation is observed in $MgAl_2O_4$ under high pressure [2]. Recently, the spinel-to-$CaFe_2O_4$-type structure transformation was found in $LiMn_2O_4$ [3]. The $CaFe_2O_4$-type $Li_{0.92}Mn_2O_4$ was synthesized by spinel-type $LiMn_2O_4$ annealed at 1100 °C in 6 GPa. The phase transition of spinel-type $LiMn_2O_4$ was occurred in above 450 °C and 1 GPa [4]. Although the magnetic properties of the $CaFe_2O_4$-type $Li_{0.92}Mn_2O_4$ have been precisely investigated, the electrochemical lithium intercalation and deintercalation properties have not been revealed. Our group has studied the electrochemical properties of $CaFe_2O_4$-type $Li_{0.81}Mn_2O_4$. This sample was obtained by Na/Li ion

* Corresponding author. AIST Central 5, 1-1-1 Higashi, Tsukuba, Ibaraki 305-8565, Japan. Tel.: +81 29 861 6817; fax: +81 29 861 4537.
E-mail address: m.mamiya@aist.go.jp (M. Mamiya).

0378-7753/$ – see front matter © 2013 Elsevier B.V. All rights reserved.
http://dx.doi.org/10.1016/j.jpowsour.2013.01.159

exchange from the high-pressure synthesized $CaFe_2O_4$-type $NaMn_2O_4$ [5]. The material shows a discharge capacity shows 113.3 mAh g^{-1} in the range of 4.8–3.0 V (vs Li/Li+).

Transition metal substitution in spinel-type $LiMn_2O_4$ is one of the ways to improve the electrochemical properties. For instance, spinel-type $LiMn_{2-x}Ni_xO_4 (0 < x < 0.5)$ increases the discharge voltage [6], and spinel-type $LiMn_{1.5}Ni_{0.4}Cr_{0.1}O_4$ showed a discharge capacity of 131 mAh g^{-1} (vsLi/Li+) in the range of 5.0–3.0 V [7].

$CaFe_2O_4$-type $LiMn_2O_4$ is thought to be useful in order to improve the electrochemical properties by transition metal substitutions. Previously, we have synthesized the high-pressure phase of $Li_xTi_2O_4$ [8]. The sample has intergrowth structure between $CaFe_2O_4$-type and Ramsdellite-type Ti_2O_4 layers, alternatively. The $CaFe_2O_4$-type $Li_xTi_2O_4$ has not been synthesized, yet. Although, the cycle performance is better than the Ramsdellite-type TiO_2.

In this work, we have synthesized the $CaFe_2O_4$-type $Li_x(M_{0.1}Mn_{0.9})_2O_4$ (M = Ni, Ti) and analyzed the crystal structures. Furthermore, we measured the electrochemical properties and discussed the effect of transition metal substitution in the $CaFe_2O_4$-type $LiMn_2O_4$.

2. Experimental procedure

Transition metal substituted $CaFe_2O_4$-type $Li_x(M_{0.1}Mn_{0.9})_2O_4$ (M = Ni, Ti) was synthesized by the same way like $CaFe_2O_4$-type $LiMn_2O_4$. Details of the procedure were described in elsewhere [5].

Transition metal substituted $CaFe_2O_4$-type $Li_x(M_{0.1}Mn_{0.9})_2O_4$ (M = Ni, Ti) was synthesized by Na/Li ion exchange from high-pressure synthesized $CaFe_2O_4$-type $Na(M_{0.1}Mn_{0.9})_2O_4$. The powdered reagents of Na_2O_2, MnO_2 and NiO or TiO_2 were mixed into the target ratio. The mixture was put into a cubic-anvil type high-pressure apparatus and heated at 1273 K for 1 h under a pressure of 4.5 GPa. Na/Li ion exchange was carried out by soaking the molten $LiNO_3$ at 633 K for 12 h.

The phase purity and crystal structure were characterized by powder X-ray diffraction (XRD) (Rigaku RINT). The XRD intensity data for the Rietveld analysis were collected for 4 s at each 0.02° step over a 2-theta range from 10 to 80° under Cu Kα radiation with 40 kV, 200 mA. The program of RIETAN-FP [9] was used for the Rietveld analysis.

Electrochemical lithium intercalation/deintercalation experiments were performed using lithium coin-type cells. The working electrode was prepared by mixing 45% active material, 45% acetylene black and 10% polytetrafluorothylene (PTFE) powder in weight by pressing the mixture onto an Al mesh having a diameter of 15 mm under a pressure of 20 MPa. The electrochemical test cells were constructed in an aluminum coin type configuration. The counter electrode was a Li foil having a diameter of 15 mm. The separator was piled up a micro glass fiver filter and a micro porous polypropylene sheet having diameters of 15 mm each. A solution of 1 M $LiPF_6$ in a 50:50 mixture of ethylene carbonate (EC) and diethylcarbonate (DEC) by volume (Kishida Chemical Co. Ltd.) was used as the electrolyte. Cells were constructed in an argon-filled glove box, and electrochemical measurements were carried out with a current density of 10 mA g^{-1} at 25 °C.

3. Results and discussion

Black colored powdered samples were obtained. About 0.5 g amount of sample was synthesized by one batch.

The reaction products of $Li_x(Ni_{0.1}Mn_{0.9})_2O_4$, $Li_x(Ti_{0.1}Mn_{0.9})_2O_4$ and $Li_{0.81}Mn_2O_4$ were examined by powder X-ray diffraction (XRD). Fig. 1 shows the XRD patterns of the products. All peaks are assigned to the single phases having $CaFe_2O_4$-type structure. The products were synthesized by Na/Li ion exchange from

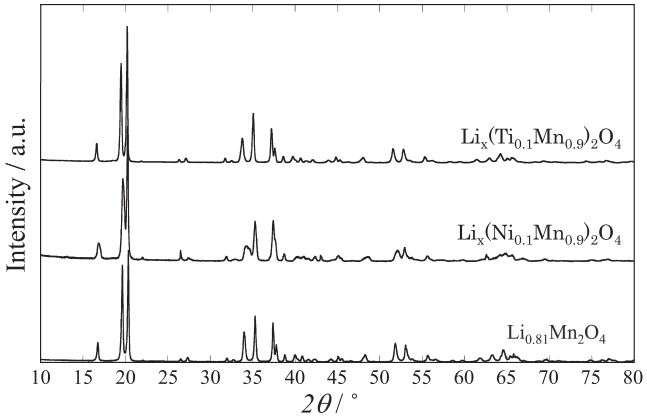

Fig. 1. XRD patterns of $CaFe_2O_4$-type $Li_{0.81}Mn_2O_4$, $Li_x(Ni_{0.1}Mn_{0.9})_2O_4$ and $Li_x(Ti_{0.1}Mn_{0.9})_2O_4$.

$Na(M_{0.1}Mn_{0.9})_2O_4$ (M = Ni, Ti). The results shows the Na/Li ion exchanges are completed in the all sample.

The crystal structures were analyzed by Rietveld method using XRD data. Fig. 2 shows the observed, calculated and difference patterns of the $Li_x(Ni_{0.1}Mn_{0.9})_2O_4$ and $Li_x(Ti_{0.1}Mn_{0.9})_2O_4$. In the analysis, the population of Li was assumed to be 1. The structure parameters are summarized in Table 1a and b. The lattice parameters of $Li_x(Ni_{0.1}Mn_{0.9})_2O_4$ are a = 8.619(2), b = 2.28117(7), c = 10.294(5) Å and $Li_x(Ti_{0.1}Mn_{0.9})_2O_4$ are a = 8.657(2), b = 2.819(14), c = 10.482(4) Å. The lattice parameters $Li_{0.81}Mn_2O_4$ are a = 8.7321(13), b = 2.84983(6), c = 10.5700(2) Å [5]. The lattice parameters of the substituted samples are smaller than the values of $Li_{0.81}Mn_2O_4$.

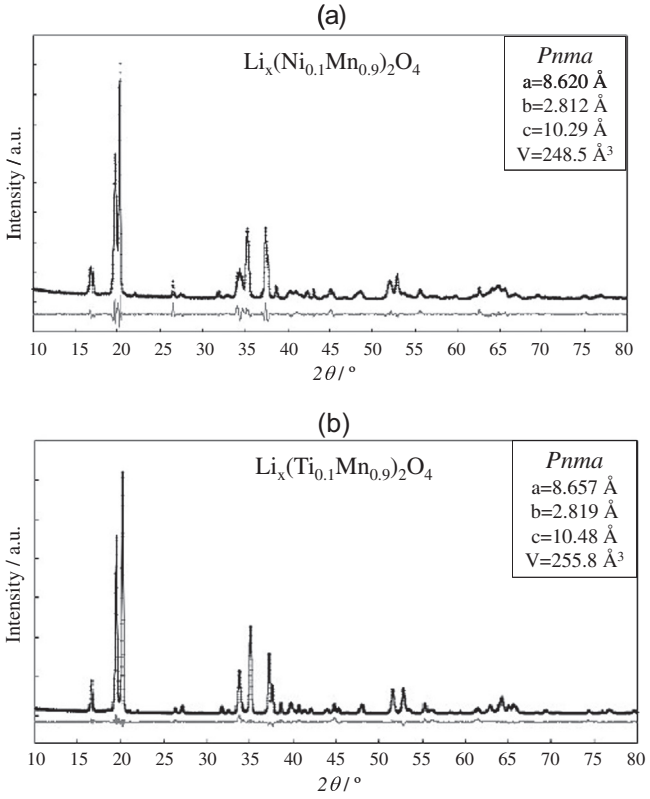

Fig. 2. Observed (plus marks), calculated (solid line) and difference (gray line) patterns for the Rietveld analysis from the powder X-ray diffraction data of (a) $Li_x(Ni_{0.1}Mn_{0.9})_2O_4$ and (b) $Li_x(Ti_{0.1}Mn_{0.9})_2O_4$.

Table 1a
Atomic positional and equivalent isotropic displacement parameters for $Li_x(Ni_{0.1}Mn_{0.9})_2O_4$.

Atom	x	y	z	B	Population
$Li_x(Ni_{0.1}Mn_{0.9})_2O_4$					
Li	0.267(6)	0.25	0.34(16)	13(1)	1
Mn1	0.0558(16)	0.25	0.1142(4)	1.51(7)	0.851(6)
Ni1	0.0558(16)	0.25	0.1142(4)	1.51(7)	0.149(6)
Mn2	0.0849(5)	0.25	0.6021(5)	1.51(7)	0.949(6)
Ni2	0.0849(5)	0.25	0.6021(5)	1.51(7)	0.051(6)
O1	0.3079(4)	0.25	0.6549(3)	0.84(8)	1
O2	0.3946(8)	0.25	0.9861(7)	0.84(8)	1
O3	0.4614(7)	0.25	0.2089(9)	0.84(8)	1
O4	0.0617(3)	0.25	0.929(17)	0.84(8)	1

$R_{wp} = 9.46\%$, $s = 2.37$.

Table 1b
Atomic positional and equivalent isotropic displacement parameters for $Li_x(Ti_{0.1}Mn_{0.9})_2O_4$.

Atom	x	y	z	B	Population
$Li_x(Ti_{0.1}Mn_{0.9})_2O_4$					
Li	0.247(3)	0.25	0.354(3)	13(1)	1
Mn1	0.0605(3)	0.25	0.1168(3)	2.09(7)	0.995(3)
Ti1	0.0605(3)	0.25	0.1168(3)	2.09(7)	0.004(3)
Mn2	0.0839(3)	0.25	0.6004(2)	2.09(7)	0.804(3)
Ti2	0.0839(3)	0.25	0.6004(2)	2.09(7)	0.195(3)
O1	0.3079(6)	0.25	0.6425(6)	1.6(18)	1
O2	0.3812(5)	0.25	0.9913(6)	1.6(18)	1
O3	0.4651(7)	0.25	0.1931(5)	1.6(18)	1
O4	0.0644(6)	0.25	0.9138(5)	1.6(18)	1

$R_{wp} = 9.76\%$, $s = 2.73$.

Fig. 3 illustrates schematic crystal structures of the $CaFe_2O_4$-type $LiMn_2O_4$. The structure has one dimensional tunnel structures consisting edge-shared MnO_6 octahedron. There are two Mn sites, Mn(I) and Mn(II). Major Ni substitution takes place at Mn(I) site, on the other hand almost all Ti substitution takes place at Mn(II) site. The substitution rates are summarized in Table 2. The valence numbers of Ni and Ti are estimated as 2+ and 4+. After the substitutions, the valence number of Mn(I) is decreased in $Li_x(Ni_{0.1}Mn_{0.9})_2O_4$, on the other hand the number of Mn(II) is increased in $Li_x(Ti_{0.1}Mn_{0.9})_2O_4$. The tunnel structures are formed by edge shared MnO_6 octahedrons. The volume of MnO_6 octahedrons are 2% reduced in Mn(I) site and 8% reduced in Mn(II) site in the Ni substituted one, and no change in Mn(I) site and 9% reduced in Mn(II) site in the Ti substituted one. When the lithium populations were calculated from the 1st charge capacities, the x value were supposed to be 0.86 in $Li_x(Ni_{0.1}Mn_{0.9})_2O_4$ and $x = 0.71$ in $Li_x(Ti_{0.1}Mn_{0.9})_2O_4$. The populations are not significant difference compared with $Li_{0.81}Mn_2O_4$. The volumes of Mn sites to be reduced are the main factor of contraction of whole unit cells.

Fig. 4 shows the initial Li-on insertion and deinsertion profile of the $Li_x(Ni_{0.1}Mn_{0.9})_2O_4$, $Li_x(Ti_{0.1}Mn_{0.9})_2O_4$ and $Li_{0.81}Mn_2O_4$ in the

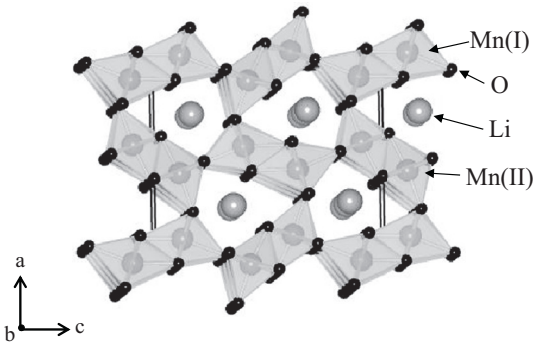

Fig. 3. Schematic illustrations of crystal structure of $Li_{0.81}Mn_2O_4$.

Table 2
The substitution rates of Ni and Ti at the Mn-sites of $CaFe_2O_4$-type $LiMn_2O_4$.

$Li_x(Ni_{0.1}Mn_{0.9})2O_4$		$Li_x(Ti_{0.1}Mn_{0.9})2O_4$	
Mn(I)	Mn: 85.1 Ni: 14.9	Mn(I)	Mn: 99.5 Ti: 0.5
Mn(II)	Mn: 94.9 Ni: 5.1	Mn(II)	Mn: 80.5 Ti: 19.5

voltage range between 4.8 and 3.0 V (vs Li/Li^+) at a current density of 10 mA g^{-1} at 25 °C.

There are two plateaus at 3.7 and 2.6 V in the discharge profile of $Li_{0.81}Mn_2O_4$. The two plateaus correspond to the redox reaction of Mn in the Mn(I) site at 3.7 V and Mn(II) site at 2.6 V, respectively. However, the crystal structure is not stable after the lower plateau. High cycle performance shows only the range set above 2.6 V [5].

In this work, the measurement range was set between 4.8 and 3.0 V. The range means the electrochemical properties are focused by the redox reaction at Mn(I) site.

The initial discharge capacities and average voltages were as follows; $Li_x(Ni_{0.1}Mn_{0.9})_2O_4$ is 119.3 mAh g^{-1} and 3.93 V, $Li_x(Ti_{0.1}Mn_{0.9})_2O_4$ is 122.0 mAh g^{-1} and 3.65 V, $Li_{0.81}Mn_2O_4$ is 113.3 mAh g^{-1} and 3.72 V.

There is a flat potential plateau at 3.7 V in the profile of $Li_x(Ti_{0.1}Mn_{0.9})_2O_4$ and $Li_{0.81}Mn_2O_4$. The discharge profile of $Li_x(Ti_{0.1}Mn_{0.9})_2O_4$ and $Li_{0.81}Mn_2O_4$ are similar. The crystal structure analysis indicates only 2.5% Ti substituted Mn at Mn(I) site and another Ti substituted at Mn(II) site. The energy density of $Li_x(Ti_{0.1}Mn_{0.9})_2O_4$ is 445.30 Wh kg^{-1}, which is 5.6% higher than the value of $Li_{0.81}Mn_2O_4$.

On the other hand, the discharge profile of $Li_x(Ni_{0.1}Mn_{0.9})_2O_4$ is different. The profile shows simple slope down without any plateaus. The crystal structure analysis indicates 74.5% Ni substitution has occurred at Mn(I) site. The redox reaction of Mn and Ni should occur, simultaneously. The Ni redox reaction is effective for increase the discharge voltage. The energy density of $Li_x(Ni_{0.1}Mn_{0.9})_2O_4$ is 453.84 Wh kg^{-1}, which is 9.8% higher than the value of $Li_{0.81}Mn_2O_4$.

Fig. 5 shows the cycle performance of charge–discharge properties of $Li_x(Ni_{0.1}Mn_{0.9})_2O_4$ and $Li_{0.81}Mn_2O_4$. $Li_{0.81}Mn_2O_4$ keep good cycle performance until 50 cycles. $Li_x(Ni_{0.1}Mn_{0.9})_2O_4$ is keep simple slope down discharge profiles except near the start point. When the cycle number increased, the slopes are rapidly go down and an inflection point arises around 4.5 V. The inflection point becomes clear with increasing the number of cycles. The average discharge voltage and capacity also go down. After 50 cycles, the discharge

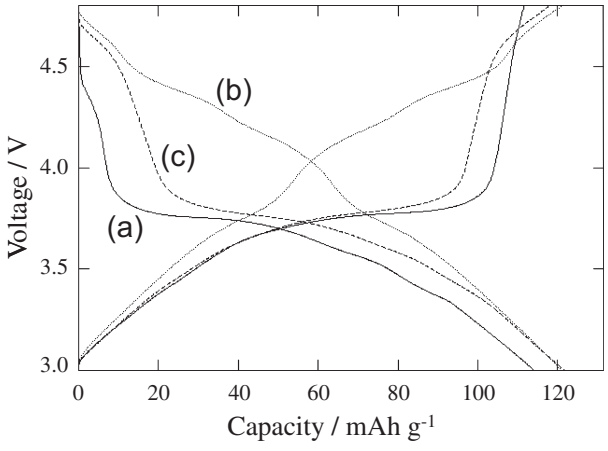

Fig. 4. Initial electrochemical Li-ion intercalation and deintercalation profiles for (a) $Li_{0.81}Mn_2O_4$, (b) $Li_x(Ni_{0.1}Mn_{0.9})_2O_4$ and (c) $Li_x(Ti_{0.1}Mn_{0.9})_2O_4$.

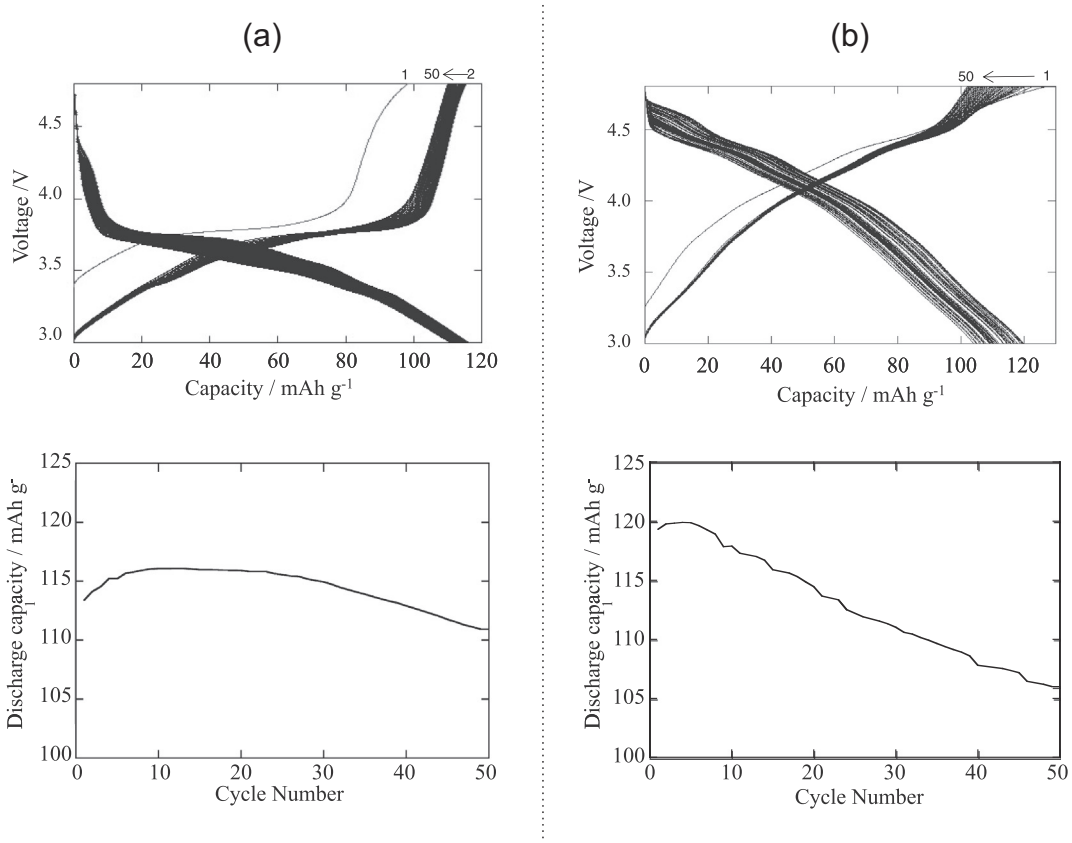

Fig. 5. Long term lithium charge–discharge cycling performance of (a) $Li_{0.81}Mn_2O_4$ and (b) $Li_x(Ni_{0.1}Mn_{0.9})_2O_4$.

capacity and voltage of $Li_x(Ni_{0.1}Mn_{0.9})_2O_4$ are 106.00 mAh g^{-1} and 3.93 V. The energy density is 416.58 Wh kg^{-1}, which is 11.1% lower than the initial value. On the other hand, the values of $Li_{0.81}Mn_2O_4$ are 110.93 mAh g^{-1} and 3.58 V. The energy density is 397.13 Wh kg^{-1}, which is 5.78% lower than the initial value.

Ni substitution is disadvantageous for the cycle performance, although the energy density is higher than the value before substitution. The low valence number of Ni should be unstable in Mn(I) site, as long as the redox reaction takes place here. On the other hand, in case of Ti, the structure remains stable due to unchanged in Mn(I) site.

4. Conclusions

The $CaFe_2O_4$-type $Li_{0.81}Mn_2O_4$ is a high performance positive electrode material. This study is a first attempt to improve the electrochemical property by transition metal substitutions. The substituted samples can be obtained by same synthesis way of $CaFe_2O_4$-type $Li_{0.81}Mn_2O_4$. Ni and Ti substitutions increase the discharge voltage. Ni substitution is more effective than Ti. Transition metal substitutions have occurred selectively. Mn(I) site is preferred to low valence number metals, on the other hand Mn(II) site is preferred to high valence number metals. The substitution will apply to other transition metals. High performance electrode materials will be synthesized by developing the substitutions.

Acknowledgments

This work was financially supported from the New Energy and Industrial Technology Development Organization (NEDO) in Japan (FY2007 - FY2011).

References

[1] M.M. Thackeray, Prog. Solid State Chem. 25 (1997) 1.
[2] T. Irifune, K. Fujino, E. Ohtani, Nature 349 (1991) 409.
[3] K. Yamaura, Q. Huang, L. Zang, K. Takada, Y. Baba, T. Nagai, Y. Matsui, K. Kosuba, E. Takayama-Muromachi, J. Am. Chem. Soc 128 (29) (2006) 9448.
[4] J. Darul, W. Nowicki, C. Lathe, P. Piszora, Radiat. Phys. Chem. 80 (2011) 1014.
[5] M. Mamiya, K. Kataoka, S. Kikuchi, K. Tokiwa, J. Akimoto, in preparation.
[6] Y. Wei, K.B. Kim, G. Chen, Electrochim. Acta 51 (2006) 3365.
[7] R.K. Katiyar, R. Singhal, K. Asmar, R. Valentin, R.S. Katiyar, J. Power Sources 194 (2009) 526.
[8] M. Mamiya, K. Kataoka, S. Kikuchi, K. Tokiwa, J. Akimoto, J. Phys. Chem. Solids 73 (2012) 1460.
[9] F. Izumi, K. Momma, Solid State Phenom. 130 (2007) 15.